Accurate variational Quantum Eigensolvers

Malay Singh

Supervisors : Msc Ramiro Sagastizabal and Dr. Leonardo Di Carlo
Department of Applied Physics

Delft University of technology

Three Month Report

Abstract

Put your abstract or summary here, if your university requires it.

Contents

List of Figures

LIST OF FIGURES

List of Tables

LIST OF TABLES

1

Project Proposal

One of the proposed powerful applications for near-term quantum computers is to address problems in quantum simulation of molecular structures and condensed matter physics problems, which currently stretch the limits of existing high-performance computing infrastructure[1]. In the near term quantum devices will lack the resources for full fault tolerance and therefore will be significantly error prone. Algorithms on Hybrid quantum-classical systems such as Variational quantum eigensolvers have been implemented to solve for the ground state energy of a molecular hamiltonian mapped onto a system of qubits. They require a shallow circuit for variational state preparation whose output is fed into a classical supervising algorithm. The use of many iterations of shallow circuits helps achieve lower error rates in energy estimate as compared to quantum phase estimation algorithm. For the ground state energy estimate produced by any algorithm to be useful to make realistic chemical predictions, the estimate must be within chemical accuracy of the actual ground state energy. Reaching this accuracy in quantum simulations with VQEs will require additional error mitigation strategies.

In this project we aim to experimentally study error mitigation strategies which enhance the accuracy of energy estimate. The first technique uses a further entangling $SU(4)$ operation after a state preparation step to generate a parity check along with the evaluation of pauli terms. We call it the T_1 error signalling circuit. The second technique involves running the quantum circuits for variable times, this done by adding waiting gates after every gate operation in the state preparation states. The energy estimates as a function of circuit length are fit to a polynomial and then extrapolated to the zero circuit length, the corresponding energy estimate is the refined energy estimate.

We see that this energy estimate is much more accurate as the extrapolation has the effect of tuning out errors caused by small T_1 and T_2.

We support our claims with simulations in which the quantum state preparation part is done using the quantumsim simulator developed by Brian Tarasinski. The classical optimization is done using the Nelder-Mead algorithm from the $PycQED\_py3$ software developed at the Di Carlo lab.

2

Superconducting Qubits

2.1 Quantum Information

Figure 2.1: Bloch Sphere visualisation of a single qubit state.

2.2 Superconducting Qubits

(a) Effective Circuit for the transmon qubit

(b) Energy levels for the transmon qubit for $\frac{E_J}{E_C} =?$ found by simulation.

2.2.1 Circuit Quantum Electrodynamics

2.2.2 Single and Two qubit gates

2.2.3 Readout

Figure 2.3: The transmission profile of the resonator is shifted to one of two peaks conditioned on the states of the qubit.

2.2.4 Noise

3

Quantum Simulations with Superconducting Qubits

3.1 Introduction

3.2 Hydrogen Hamiltonian

Figure 3.1: A Flowchart depicting the steps used in mapping Real Space Molecular Hamiltonian on to Qubit Hilbert space.

Figure 3.2: The dissociation curve for Hydrogen molecule.

3.3 Variational Quantum Eigensolvers

Figure 3.3: Hardware and software schematic of the variational quantum eigensolver.

4

State preparation Ansatze

4.1 Hardware oriented Ansatz

4.2 Six parameter circuit

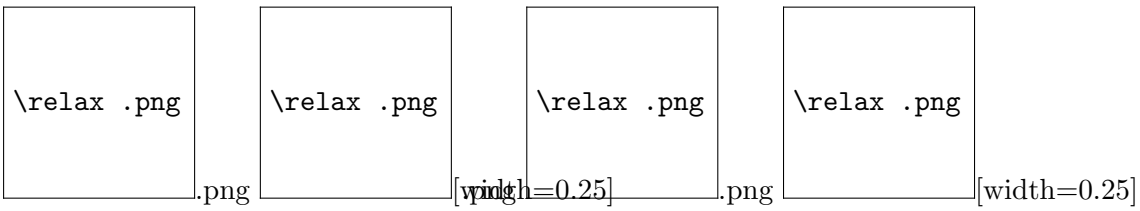

Figure 4.1: a. Quantum circuit for the six-parameter Ansatz b. Plot of Converged Energies(Hartree) across interatomic distances.

4.3 Particle number conserving circuit

The basic idea behind the particle number conserving ansatz is that we can find the solution to the ground state of the hydrogen hamiltonian by exploring a smaller hilbert space which has all the states with odd parity or only one excitation.

$$\mathcal{H}_{SE} = \text{span}\left\{|01\rangle, |10\rangle\right\} \tag{4.1}$$

$$\langle\Psi|ZZ|\Psi\rangle_{|\psi\rangle\in\mathcal{H}_{SE}} = -1 \tag{4.2}$$

In figure 4.2 (a) we propose a circuit which prepares an ansatz of the form $\cos(\theta)\,|01\rangle - i\sin(\theta)\exp(i\phi)\,|10\rangle$ using a parameterizable iSWAP gate. The concurrence

C of this state is dictated by the angle of the iSWAP and is given by $\sin(2\theta)$. In figure 4.2(b) which reports the error in converged energies across the entire dissociation curve.

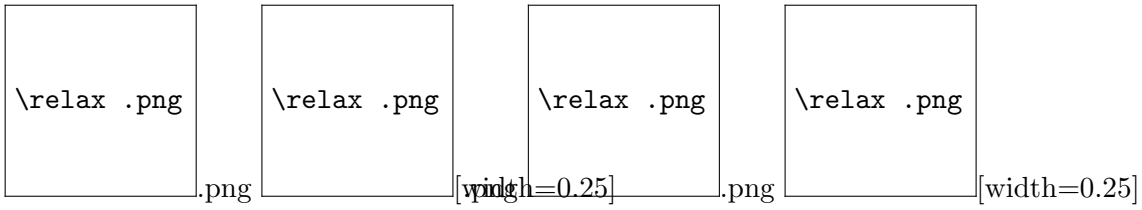

Figure 4.2: a. Quantum circuit for the particle number conserving Ansatz b. Plot of Converged Energies(Hartree) across interatomic distances.

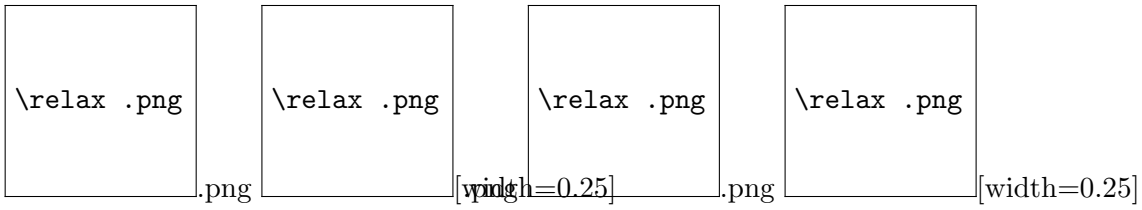

Figure 4.3: a. Converged Parameters across interatomic distances b. Plot of Concurrence of the converged state across interatomic distances.

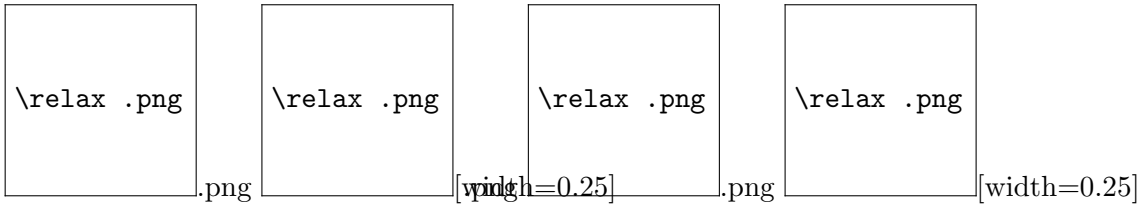

Figure 4.4: a. Landscape accesible to the optimizer, Energy as a function of θ_1 and ϕ. b. Zoom in of the landscape showing converged ground state energy.

5

Error Signalling Circuit

Inaccuracies in the ground state estimate produced by the VQE are caused due several factors most prominent of them are inaccuracy in the design of state preparation Ansatz, qubit state decay due to limited relaxation time (T_1), decay of coherence due to limited dephasing time (T_2), single qubit gate errors and two-qubit gate errors. In this section we focus on combating errors intoduced by qubit state decay. If during the preperation of the ansatz in the SPES a T_1 decay event occurs, then the state is no longer in the SPES, i.e. upon parity measurement we get a $+1$. In order for us to improve our energy estimate we must rule out states with an odd parity while simulataneously measuring pauli terms in the hydrogen hamiltonian. The hydrogen hamiltonian is given by eqn. and all terms commute with the parity operator.

$$[\, ZZ,\, IZ\,] = [\, ZZ,\, ZI\,] = [\, ZZ,\, XX\,] = [\, ZZ,\, YY\,] = 0 \tag{5.1}$$

This is the first step in ensuring that terms in the hamiltonian and parity of the state are simultaneously measurable. To measure the term $\langle XX \rangle$ we perform a two qubit clifford rotation that takes $\langle XX \rangle$ and $\langle ZZ \rangle$ to seperate qubits. After the state preperation step similar to particle number conserving circuit, we rotate both qubits to XX basis by applying $\hat{R}_{\hat{y}}(\frac{\pi}{2})$ on both qubits. We follow this with a CNOT gate

The circuit in figure 5.1(a) implements this Clifford rotation.

To verify whether

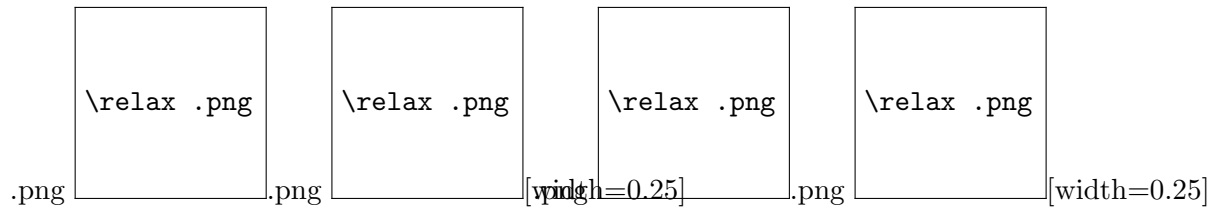

Figure 5.1: a. Plot of the quantum circuit for T_1 error signalling . b. Error as a function of distance for T_1 signalling circuit.

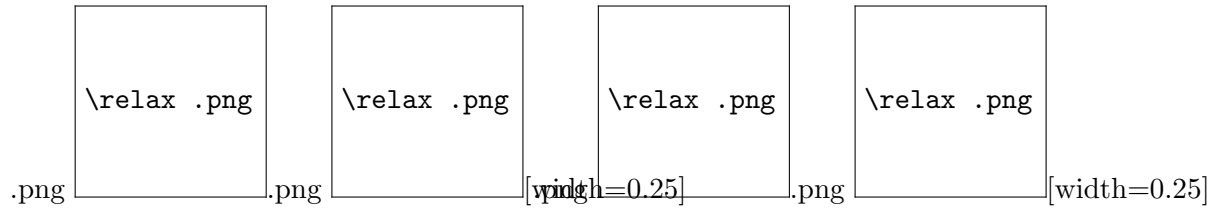

Figure 5.2: a. Plot of error vs. distance for increasing T_1 at constant T_ϕ for T_1 error signalling circuit and bare VQE circuit. b. Plot energy landscapes as a function of

6

Active Error minimization

6.1 Theory

Errors in VQE state preperation have the effect of increasing the measured expectation value of energy ($\tilde{E}$) from its true value (E). In the presence of errors the prepared state will be better represented by an ensemble given by a density matrix $\rho(\theta)$. In the ideal case when preparation is error free $\rho(\theta) = |\psi(\theta)\rangle \langle\psi(\theta)|$. The ground state variational pricnciple still exists for all values of $\overrightarrow{\theta}$.

$$\left\langle \hat{H} \right\rangle_{\rho(\overrightarrow{\theta})} \equiv \left\langle \hat{H} \right\rangle (\overrightarrow{\theta}) = Tr[\rho(\overrightarrow{\theta})\hat{H}] \geq E_{GS} \; \forall \; \theta \tag{6.1}$$

We denote the minimized energy or the energy estimate as $\tilde{E}$ and the error in energy estimate as ϵ.

$$\min_{\forall \overrightarrow{\theta}} \left\langle \hat{H} \right\rangle_{\rho(\overrightarrow{\theta})} \equiv \tilde{E} \tag{6.2}$$

$$\epsilon \equiv \mid \tilde{E} - E_{GS} \mid \tag{6.3}$$

The basic idea behind active error minimization is that we want to have parameter(s) λ which characterize the errors in our Energy estimation. We then find a functional relationship between the Energy estimate and the error parameter. We extrapolate this curve to $\lambda \to 0$ and find $\tilde{E}(\lambda \to 0)$. This technique works only in the case when the errors in the state preperation are stochastic, such that the operation is described by a superoperator $\hat{N}\hat{U}(\theta)$ and $\hat{N}$ can be written as:

$$\hat{N}_\lambda = (1 - \lambda)\hat{I} + \lambda\hat{E} \tag{6.4}$$

Where $\hat{U}(\theta)$ is the ideal unitary operator used to prepare the state ansatz, $\hat{N}$ is a superoperator describing the effect of noise, $\hat{I}$ is an identity operation and errors $\hat{E}$ occur with a probability λ. Starting with an initial state $|0\rangle\langle 0|$, after n iterations of state preperation, the density matrix obtained is given by:

$$\rho_\lambda(\overrightarrow{\theta_n}) = \hat{N}_{n,\lambda}\hat{U_n}..\hat{N}_{1,\lambda}\hat{U_1}\,|0\rangle\langle 0| \tag{6.5}$$

Where the ideal unitary operator in the l^{th} iteration is given by $\hat{U}(\theta_l)$. Taking into account that the errors are stochastic, the minimized outcome of expectation value of the hamiltonian can be written as:

$$\left\langle \hat{H} \right\rangle_{\rho_\lambda} = (1 - r\sum_l \lambda_l)\left\langle \hat{H} \right\rangle^{(0)}_{\rho^{(0)}} + r\left\langle \hat{H} \right\rangle^{(1)}_{\rho^{(1)}} + O(r^2) \tag{6.6}$$

Here, $\left\langle \hat{H} \right\rangle_{\rho_\lambda} = Tr[\hat{H}\rho_r(\overrightarrow{\theta})]$ and $\left\langle \hat{H} \right\rangle^{(0)}_{\rho^{(0)}} = Tr[\hat{H}\rho^{(0)}(\overrightarrow{\theta})]$ and $\rho^{(0)} = \hat{U}_n...\hat{U}_1$ i.e. the density matrix without any errors. $\rho^{(1)} = r\sum_l \lambda_l \hat{U}_n...\hat{E}_l\hat{U}_l...\hat{U}_1(|0\rangle\langle 0|)$ denotes the normalized sum of all state preperation density matrices in which in which only one of the operations causes an error, and all other operations are ideal. Note, that in these equations r is a scale factor and we have replaced the error probability λ_l with $r\lambda_l$ allowing us to write eqn(6.6) with r dependence on the right hand side. The value $\left\langle \hat{H} \right\rangle^{(0)}_{\rho^{(0)}}$ is the true value of energy estimate and can by obtained by the means of extrapolation. The equation below makes it clear:

$$\left\langle \hat{H} \right\rangle^{(0)}_{\rho_r} = \left\langle \hat{H} \right\rangle^{(0)}_{\rho^{(0)}} + \chi r \tag{6.7}$$

In our experiments the error parameters r cannot be less than r_{min} therefore to access the true value of energy estimate, we increase r and extrapolate energy estimate to $r = 0$.

6.2 Simulations

To ascertain the usefulness of the active error minimization protocol we begin by constructing a protocol to tune out errors introduced in our circuit by finite decay and pure dephasing characterized by T_1 and T_ϕ respectively. In our experiments it is not feasible to change either of these numbers. But since total errors per evaluation of the

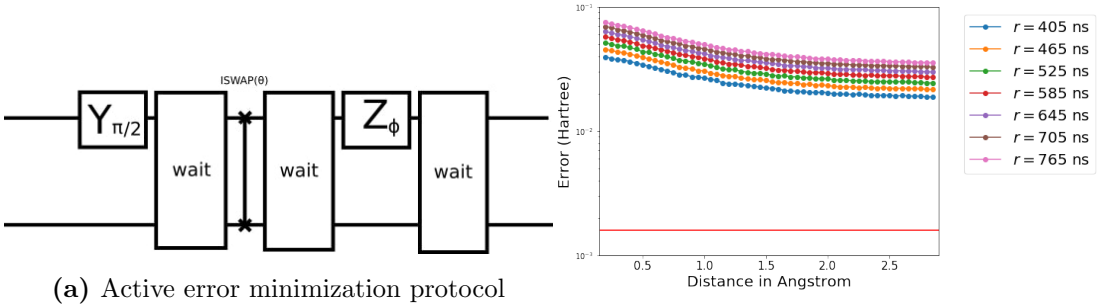

(a) Active error minimization protocol

(b) Errors vs. distance for variable circuit lengths(τ)

Figure 6.1: Errors in energy estimate for increasing circuit lengths(r).(a) A waiting gate is inserted after every gate operation, the $r = 405$ ns without any waiting gate. This includes 300 ns of measurement time(not shown). The waiting times are added in steps of 20 ns.(b) Error in energy estimation for various r. The simulation is done with $T_1 = 25\mu$s and $T_2 = 40\mu$s

circuit is just an integration of the rate of errors over time of exposure, so we instead change the circuit length by adding waiting gates(Fig 6.1 (a)) after every gate operation thereby changing the time for which our system is exposed to decoherence. We obtain error in energy estimation for the entire dissociation curve for several values of waiting time(Fig 6.1(b)). The total circuit length which becomes our parameter "r" is related to waiting times by the equation r = native circuit length + 3×wait time. The native circuit length includes an extra 300ns of waiting gate, to account for decoherence effects during the measurement apart from single qubit and two qubit gate lengths of 25 and 50ns respectively. We observe an increase in the errors with increasing circuit length.

In Fig 6.2 (a) we look at errors in energy estimation for the Hydroden Hamiltonian at an interatomic distance of 0.7$\mathring{A}$. We see a linear trend which we fit, it's intercept with the Y-axis gives us $\left\langle \hat{H} \right\rangle^{(0)}_{\rho^{(0)}} = 1.13$mHartree. We call this the zero noise limit as it corresponds to the hypothetical case in which all gate operations were performed instantaneously so that there was no exposure to decoherence during them, and these operations had no additional errors. Note that the decoherence during measurement is still introducing errors in the energy estimate. We see a considerable improvement in our energy estimate for the entire dissociation curve in comparison to bare VQE. We must emphasize that our error model is limited to decay and pure dephasing, which is far from true. We discuss the limitations of the simulations briefly in the next section.

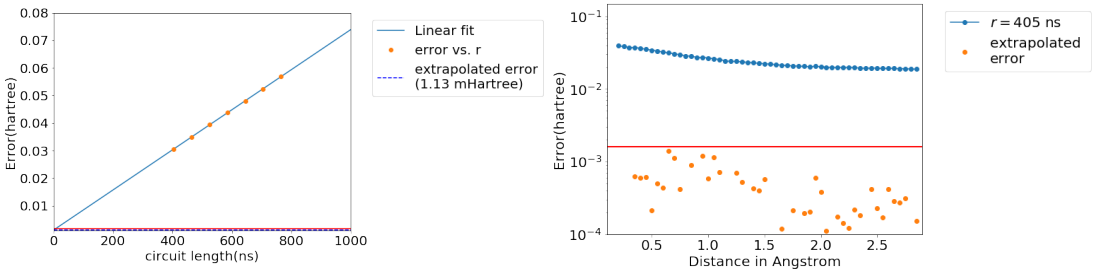

(a) Linear fit of errors vs. r

(b) Improvement in the energy estimate

Figure 6.2: Improvement in energy estimate by extrapolation to zero circuit length.(a)The extrapolated error (dashed blue line) for the Hydrogen Hamiltonian at the interatomic distance $0.7\mathring{A}$ (b) Errors for the entire dissociation curve with and without Active error minimization.

6.3 Limitations of the simulations

7

Outlook

7.1 Experience Gained

7.1.1 Oscilloscope Driver

7.1.2 Quantum State Tomography

7.1.3 Miscellaneous

7.2 Experience Necessary

8

Simulations using quantumsim